Quantum Three-Phase Power Flow Integrating Unbalanced Grid-Forming IBRs

Kamini Shahare, Fei Feng, Yacov Shamash, and Peng Zhang

***Abstract*—Three-phase unbalanced power flow analysis is essential for distribution system operations, but its computational complexity poses a challenge for future large-scale real-time applications. This paper devises a unbalanced three-phase power flow that integrate hierarchically controlled GFM. The main contribution include: 1) a droop-controlled three phase Newton power flow algorithm which incorporated the droop characteristics of GFM; 2) a secondary-controlled three phase power flow method for power sharing and voltage regulations; 3) integrate a Variational Quantum Linear Solver (VQLS) into the Newton step power flow, replacing the classical linear solver with a Hermitian-embedded, variational solution amenable to near-term quantum devices. On the IEEE 4- node unbalanced feeder, the quantum-augmented three-phase power flow achieves the same voltage profiles and droop-controlled behavior as the classical solver while enabling diagnostics of linear residual and mismatch convergence.**

***Index Terms*—unbalanced, distribution network, power flow, GFM, quantum, VQLS**

I. INTRODUCTION

The growing complexity of the grid and tighter operational margins motivate scalable numerical methods for planning and operation. Distribution feeders are increasingly unbalanced and populated with inverter-based resources (IBRs), making robust and scalable three-phase power flow a persistent need. Thus, three-phase unbalanced power flow analysis is a critical need for distribution system operations [1].

At scale, AC power flow (ACPF) is dominated by repeated sparse linear solves inside Newton–Raphson or fast-decoupled iterations. Quantum linear-system solvers promise algorithmic speedups for such tasks: HHL achieves polylogarithmic scaling in problem size under sparsity and condition-number assumptions, and near-term variational approaches (VQLS) reduce circuit depth by hybridizing with classical optimizers [2]. These primitives (and broader QSVT/block-encoding frameworks) are attractive for PF's structured, sparse Jacobians and scenario ensembles. That said, any realistic claim of advantage must factor data loading, matrix block-encoding, condition numbers, and—crucially—readout of many voltage components, which can erase asymptotic gains [3]. Hence the current research arc: map PF subproblems to linear solves amenable to HHL/QSVT, and explore NISQ-friendly VQLS formulations while being explicit about I/O cost.

The "Quantum Power Flow (QPF)" line initiated HHL-based inner solves within a fast-decoupled framework by crafting Hermitian, near-constant Jacobians and demonstrated proof-of-concept accuracy on small systems [4]. Subsequent efforts tested QPF variants on real quantum backends and simulators, reported noise/scale limits, and explored hybrid or improved linear solvers. In parallel, VQLS-based PF formulations have been proposed as NISQ-amenable alternatives, and annealing-based encodings have solved PF relaxations/approximations (e.g., DC or quadratic forms) to study scalability under noise [5]. Recent critical analyses emphasize end-to-end costs (data loading, condition numbers, measurement overhead), highlighting when PF subroutines may or may not admit net quantum gains [6-7].

Despite progress, nearly all quantum PF demonstrations to date treat single-phase (DC/FDLF/positive-sequence) models. Distribution applications, however—hosting capacity, phase balancing, regulator/tap settings, EV/PV siting, and protection—demand unbalanced three-phase voltages and currents. Extending QPF to this regime introduces larger, block-structured, complex and generally non-Hermitian linear systems due to phase coupling and component models.

Thus, the main contributions of this paper are as follows:

- Proposing an unbalanced three-phase power flow formulation that augments the PF equations with primary droop and secondary control for single-phase GFM based IBRs bus instead of slack bus.
- A secondary controlled three phase power flow method for power sharing and voltage regulations
- Implementing a prototype VQLS-based Newton step, and comparing it against a classical direct solver on a 4-bus unbalanced three-phase test feeder with a single-phase GFM based IBR bus.

The remainder of this paper is organized as follows: Section I outlines the need of quantum in unbalanced three phase power flow. Section II introduces the methodology to develop unbalance three-phase power flow in quantum framework. Section III provides the experimental setup for validation, with conclusion summarized in Section IV.

This work relates to the Department of Navy award N000142512374 issued by the Office of Naval Research. The United States Government has a royalty-free license throughout the world in all copyrightable material contained herein. *Corresponding Author: Peng Zhang.*

Kamini Shahare, Peng Zhang, and Yacov Shamash are with the Department of Electrical and Computer Engineering, Stony Brook University, New York, 11794, USA (e-mail: kamini.shahare@stonybrook.edu; p.zhang@stonybrook.edu; yacov.shamash@stonybrook.edu).

Fei Feng is with the Department of Electrical Engineering, SUNY Maritime, New York, 10465, USA (email: ffeng@sunymaritime.edu).

979-8-3315-8138-1

II. METHODOLOGY

The hierarchical control for GFM consists of two schemes designed to achieve power sharing and voltage regulation for the system. Thus, control is implemented in a d-q reference frame rotating at angular speed ω. The two control schemes; droop control and secondary control for three-phase power flow are described in this section.

A. Nodal Admittance and State Vector

The network is modeled by the $3N \times 3N$ complex nodal admittance matrix $Y = G + B$, where N is the number of buses, and indices $k \in \{1, \dots, 3N\}$ map to bus-phase nodes. Each complex nodal voltage $V_k = |V_k| e^{\theta_k}$ is defined by two variables [8]. The state vector $x \in \mathbb{R}^{2N}$ comprises the voltage angles and magnitudes for all non-slack phase-nodes:

$$x = \begin{bmatrix} \theta \\ |V| \end{bmatrix} \tag{1}$$

B. Newton–Raphson Solution

The solution is found iteratively using the Newton–Raphson method by solving the linear system:

$$J\big(x^{(k)}\big)\, \Delta x^{(k)} = -F\big(x^{(k)}\big), \qquad x^{(k+1)} = x^{(k)} + \Delta x^{(k)} \tag{2}$$

The Jacobian matrix J is partitioned according to the state variables as $J = \begin{bmatrix} H & N \\ M & L \end{bmatrix}$. The off-diagonal block entries for $k \neq m$ are:

$$\frac{\partial P_k}{\partial \theta_m} = |V_k||V_m||Y_{km}| \sin(\theta_k - \theta_m - \angle Y_{km}) \tag{3}$$

$$\frac{\partial Q_k}{\partial |V_m|} = |V_k||Y_{km}| \sin(\theta_k - \theta_m - \angle Y_{km}) \tag{4}$$

The full Jacobian incorporates all partial derivatives, respecting the structure of $F(x)$ based on bus type. The diagonal terms are derived similarly, accounting for $k = m$. ZIP load dependency on $|V_k|$ is incorporated by adjusting $\partial \Delta P_k / \partial |V_k|$ and $\partial \Delta Q_k / \partial |V_k|$ as needed.

C. Single Phase GFM Controls

Let $k \in \mathcal{D}$ index IBR phases. Primary droops are

$$\Delta P_k = -\frac{1}{m_k^{pf}} (\omega_0 - \omega), \tag{5}$$

$$\Delta Q_k = -\frac{1}{n_k^{qv}} \big(V_{d,k} - V_k^{\text{eff}}\big), \tag{6}$$

with $\omega = 2\pi f$, $V_k^{\text{eff}} = |V_k - Z_{d,k} I_k|$ if a virtual impedance $Z_{d,k}$ is used; otherwise $V_k^{\text{eff}} = |V_k|$.

The GFM behaviors and corresponding J elements under three typical Secondary control loops are given as:

- Reactive Power Sharing (RPS): RPS helps to realize proportional reactive power sharing, where the VAR injection from a leader bus is updated through Q/V droop control and the rest of GFM follow. It can be given as:

$$\text{RPS:} \;\; P_{\text{bias},i} \leftarrow P_{\text{bias},i} + K_i^{\text{rps}} (\rho_i P_{\text{tot}} - P_i) \tag{7}$$

- Voltage Regulation Mode (VR): VR mode helps to recover the GFM bus voltages to their rated value by adjusting its recative power injections. Thus, the var outputs of the GFM buses and the coresponding J elements are updated [9].

$$\text{VR:} \;\; V_{d,k} \leftarrow V_{d,k} + K_k^v \left(1 - |V_k^{\text{eff}}|\right) \tag{8}$$

- Smart Tuning Mode (ST): The leader bus GFM follows the VR mode to recover back to its rated value, while other buses are adjusted for proportional recative power sharing.

$$\text{ST:} \;\; P_{\text{bias},i} \leftarrow P_{\text{bias},i} + K_i^f \, \rho_i (60 - f) \tag{9}$$

where i indexes IBRs, ρ_i are sharing weights ($\sum_i \rho_i = 1$), and $P_i = \sum_{k \in i} P_k$.

III. QUANTUM THREE-PHASE UNBALANCED POWER FLOW

To embed the real-valued system $A \Delta x = b$ into a quantum register, we pad it to dimension 2^q for some integer number of qubits q [10-11]. Let

$$q = \lceil \log_2 n \rceil, \qquad d = 2^q. \tag{10}$$

We then define

$$A_{\text{pad}} = \begin{bmatrix} A & 0 \\ 0 & 0 \end{bmatrix} \in \mathbb{R}^{d \times d}, \qquad b_{\text{pad}} = \begin{bmatrix} b \\ 0 \end{bmatrix} \in \mathbb{R}^d. \tag{11}$$

For the 4-bus case with $n = 22$, we obtain $q = 5$ and $d = 2^5 = 32$.

On q qubits, the computational basis is

$$\left\{\, |0\rangle, |1\rangle, \dots, |d-1\rangle \,\right\}, \tag{12}$$

and the initial state is the all-zero state

$$|\mathbf{0}\rangle := |0\rangle^{\otimes q}. \tag{13}$$

1) Quantum Ansatz State: We employ a parameterized ansatz $U(\theta)$ acting on q qubits, for example the `EfficientSU2` circuit from Qiskit with a chosen depth parameter. The variational state is

$$|\psi(\theta)\rangle = U(\theta)\, |\mathbf{0}\rangle = \sum_{i=0}^{d-1} c_i(\theta)\, |i\rangle, \tag{14}$$

where $c_i(\theta) \in \mathbb{C}$ are complex amplitudes satisfying

$$\sum_{i=0}^{d-1} \left| c_i(\theta) \right|^2 = 1. \tag{15}$$

In the prototype implementation, the real part of the statevector amplitudes is used as a *candidate solution* for the padded linear system. That is, we define the real-valued vector

$$x(\theta) := \Re\left\{ \mathbf{c}(\theta) \right\} \in \mathbb{R}^d, \tag{16}$$

where $\mathbf{c}(\theta) = (c_0(\theta), \dots, c_{d-1}(\theta))^\top$.

979-8-3315-8138-1

2) Cost Function: The padded linear system to be solved is

$$A_{\text{pad}}\, x = b_{\text{pad}}. \tag{17}$$

A natural least-squares objective is

$$\min_{x\in\mathbb{R}^d} \left\| A_{\text{pad}} x - b_{\text{pad}} \right\|_2^2. \tag{18}$$

In the variational approach, we restrict x to lie in the manifold generated by the quantum state $|\psi(\theta)\rangle$, and refine the objective through an additional scalar scaling.

Given a candidate vector $x(\theta)$, we compute

$$u(\theta) \;:=\; A_{\text{pad}}\, x(\theta) \;\in\; \mathbb{R}^d, \tag{19}$$

and define a scalar

$$\gamma(\theta) \;:=\; \begin{cases} \dfrac{u(\theta)^\top b_{\text{pad}}}{u(\theta)^\top u(\theta)}, & u(\theta)^\top u(\theta) > \varepsilon, \\ 0, & \text{otherwise}, \end{cases} \tag{20}$$

for a small threshold $\varepsilon > 0$. This factor $\gamma(\theta)$ minimizes, with respect to γ, the scalar least-squares quantity

$$\left\| \gamma\, u(\theta) - b_{\text{pad}} \right\|_2^2. \tag{21}$$

We then define the residual vector

$$r(\theta) \;:=\; \gamma(\theta)\, u(\theta) - b_{\text{pad}} \;\in\; \mathbb{R}^d, \tag{22}$$

and the scalar cost

$$C(\theta) \;:=\; \left\| r(\theta) \right\|_2^2 \;=\; r(\theta)^\top r(\theta). \tag{23}$$

The VQLS problem is thus formulated as

$$\boxed{\min_\theta\, C(\theta) = \min_\theta \left\| \gamma(\theta)\, A_{\text{pad}} x(\theta) - b_{\text{pad}} \right\|_2^2.} \tag{24}$$

A classical optimizer (e.g., COBYLA) iteratively updates the parameters θ to minimize $C(\theta)$, using repeated evaluations of the quantum state $|\psi(\theta)\rangle$ and the corresponding classical vector $x(\theta)$.

Quantum-state interpretation: In a more formal VQLS setting, the right-hand side vector b_{pad} can be associated with a normalized state

$$|b\rangle \;:=\; \frac{1}{\|b_{\text{pad}}\|_2} \sum_{i=0}^{d-1} (b_{\text{pad}})_i\, |i\rangle, \tag{25}$$

and the ideal solution state would satisfy

$$|x^\star\rangle \;\propto\; A_{\text{pad}}^{-1} |b\rangle. \tag{26}$$

The variational state $|\psi(\theta)\rangle$ is then optimized to approximate $|x^\star\rangle$ by minimizing a suitable cost derived from A_{pad} and $|b\rangle$. In the present prototype, these operations are simulated via statevectors and classical linear algebra.

3) Quantum Newton Step: Let $\theta^\star$ denote a (local) minimizer of $C(\theta)$. The corresponding optimized quantum state is

$$|\psi^\star\rangle \;:=\; |\psi(\theta^\star)\rangle \;=\; \sum_{i=0}^{d-1} c_i^\star\, |i\rangle, \tag{27}$$

with amplitudes $c_i^\star \in \mathbb{C}$. We extract the real-valued vector

$$x^\star \;:=\; \Re\{\mathbf{c}^\star\} \;\in\; \mathbb{R}^d, \tag{28}$$

and interpret its first n components as the approximate Newton step for the reduced system:

$$\Delta x_{\text{vqls}} \;:=\; \left(x_0^\star, \ldots, x_{n-1}^\star\right)^\top \;\in\; \mathbb{R}^n. \tag{29}$$

This vector Δx_{vqls} is then unpacked into the increments for the non-reference phase angles, the voltage magnitudes, and the frequency:

$$\Delta x_{\text{vqls}} \;\mapsto\; \left(\Delta\theta,\, \Delta V,\, \Delta f\right), \tag{30}$$

after which the Newton update

$$\theta^{(k+1)} = \theta^{(k)} + \Delta\theta, \quad V^{(k+1)} = V^{(k)} + \Delta V \tag{31}$$

is performed, with reference angles re-imposed and voltage magnitudes clipped to an admissible range (e.g., $[0.7,\, 1.3]$ p.u.).

In this way, the VQLS prototype acts as a *drop-in replacement* for the classical linear solver within each Newton iteration, providing an approximate Newton step computed via a hybrid quantum–classical variational procedure. Thus, the quantum newton steps are formulated to perform the three-phase PF for droop and secondary control.

A. Algorithm

The proposed algorithm presented in Algorithm 1 outlines a rigorous methodology for solving the three-phase power flow problem while incorporating Grid-Forming (GFM) control, with a clear provision for utilizing the Variational Quantum Linear Solver (VQLS) to accelerate the core computation. This structure leverages a nested iterative approach to decouple the fast electrical transients (inner loop) from the slower control dynamics (outer loop).

Initially, the three-phase nodal admittance matrix Y is assembled from the phase-impedance data Z_{abc} in per-unit, and the specified active/reactive injections P^{spec}, Q^{spec} are defined from the load and IBR setpoints. Then, initializes the state vector $(\theta, |V|, f)$, the active and reactive droop slopes m^{pf}, n^{qv}, and the auxiliary secondary-control states (frequency bias P_{bias} and voltage references V_d).

The outer loop represents the slow power flow secondary timescale. For each outer iteration t, an inner Newton loop refines the instantaneous steady-state solution. In each Newton step, the power fow residual r is evaluated including droop terms and current secondary biases, and a finite-difference Jacobian J is formed with reference-bus angle reduction. A simple left preconditioner D^{-1} is optionally applied, yielding the scaled linear system $D^{-1}J\,\Delta x = D^{-1}(-r)$. The `solver` flag is set to VQLS, this scaled system is encoded into the

979-8-3315-8138-1

Algorithm 1 Three-Phase VQLS QPF with GFM control

Build Y from Z_{abc} data (pu); set $P^{\text{spec}}, Q^{\text{spec}}$.
Init $\theta, |V|, f$, droop slopes m^{pf}, n^{qv}, secondary states.
for $t = 1, \ldots, T$ **do** ▷ outer: secondary
  for $k = 1, \ldots, K$ **do** ▷ inner: Newton
    Compute r with droops/biases; FD Jacobian J;
    Left precondition: $D^{-1} J \, \Delta x = D^{-1}(-r)$.
    if solver=VQLS **then**
      Build $(H, |y\rangle)$; run VQLS; obtain Δx.
    else
      Solve classically with damping; obtain Δx.
    end if
    Clip $\Delta\theta, \Delta|V|$; update $(\theta, |V|, f)$; enforce refs.
    if $\|\Delta x\|_\infty < \varepsilon$ **then break**
    end if
  end for
  Update ST/VR/RPS: $(P_{\text{bias}}, V_d) \leftarrow$ integrators.
end for

variational quantum linear solver, which returns an approximate Newton step Δx. The state is then updated with step-size clipping and reference-angle enforcement, and the inner loop terminates early if $\|\Delta x\|_\infty < \varepsilon$. After the inner Newton loop converges, the secondary controllers are updated via their integrators, adjusting P_{bias} and V_d for the next power flow outer iteration.

IV. Experimental Setup

A. Numerical Test

This section validates the effectiveness and accuracy of the proposed quantum three-phase power flow (QPF) on standard IEEE test systems. The method is verified using the IEEE 4-node unbalanced feeder with 4-wire $Z_{abc}^{(\text{mi})}$ and per-phase loads at Bus 3 for all the phases [12]. One IBR is placed at Bus 0 (i.e. Slack bus) with P–f and per-phase Q–V droops; secondary loops (ST/VR/RPS) are enabled per scenario.

The main performance metrics are:

1) voltage magnitude profile per bus;
2) Newton mismatch $\|r\|$ vs. iteration;
3) linear residual $\|J\Delta x + r\|/\|r\|$;
4) frequency deviation; and
5) for VQLS: ansatz depth, qubit count, and optimizer iterations.

QPF is implemented on an IBM quantum simulator (`IBMQ_qasm_simulator`) using Qiskit v2.1.0 and executed on a Dell laptop (2.10 GHz Intel Core i7–13th Gen) with Python 3.13.5.

B. Results

Table I shows the final power-flow results for the unbalanced three-phase system using the classical and QPF–VQLS solvers. Results are shown for phase a only. The voltage magnitude and angle at each bus match exactly for both solvers, with the same number of Newton iterations 14.

Fig. 1 shows the quantum three-phase power flow voltage magnitude at Bus 2 for phase a. Fig. 3 presents the voltage magnitude profile versus bus index for four control modes: DP, RPS, VR, and Smart Tuning (ST+VR+RPS). VR tightens the IBR-bus phase magnitudes around 1.0 p.u.; ST restores $f \to 60$ Hz; and RPS equalizes real power among IBRs (for multi-IBR cases).

TABLE I
Final power flow results for phase-a

Method	Bus	|V| (p.u.)	θ (deg)
Classical solver	1	1.000000	1.935
	2	1.002383	0.394
	3	1.017202	-1.390
	4	1.032680	-0.913
QPF–VQLS solver	1	1.000000	1.935
	2	1.002383	0.394
	3	1.017202	-1.390
	4	1.032680	-0.913

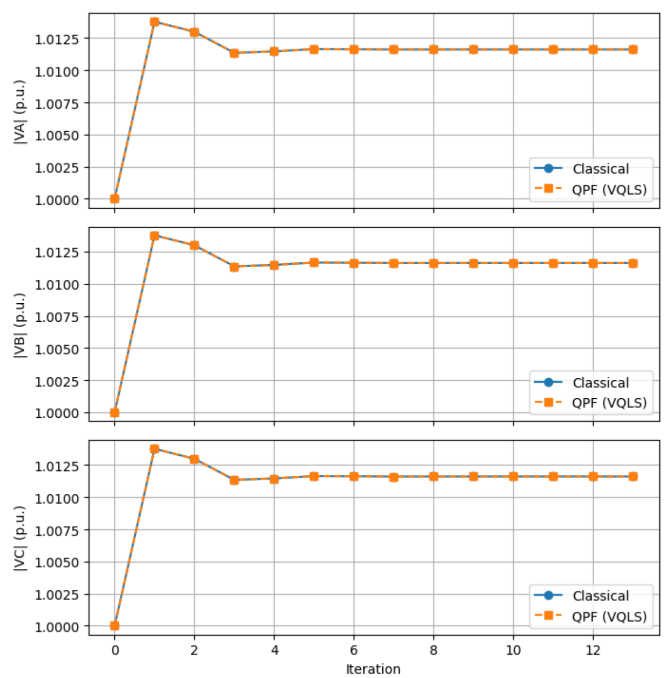

Fig. 1. Quantum three-phase voltage magnitude at Bus 2 (phase a).

Fig. 2 shows the mismatch norms $\|r\|_\infty$ and $\|r\|_2$ per Newton iteration, highlighting consistent convergence between the classical and VQLS-based solvers. Fig. 4 illustrates the probability distributions of the voltage magnitudes at Buses 2 and 4, calculated using both classical and QPF–VQLS methods.

Table II summarizes the convergence metrics for the unbalanced three-phase power flow for both the classical and QPF–VQLS solvers.

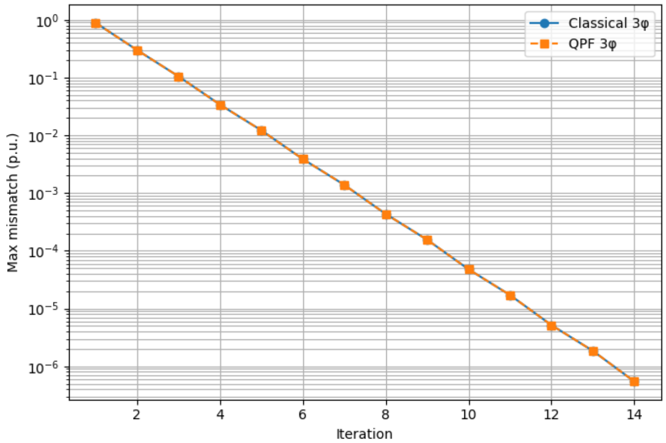

Fig. 2. Mismatch norm vs. iteration for classical and QPF–VQLS solvers.

TABLE II
CONVERGENCE SUMMARY ON IEEE 4-NODE FEEDER.

Solver	Newton iters	Final $\|r\|_\infty$	Qubits	Avg. RMSE
Classical	14	$< 10^{-8}$	–	–
VQLS (reps=2)	14	$< 10^{-8}$	5	$\leq 8 \times 10^{-8}$

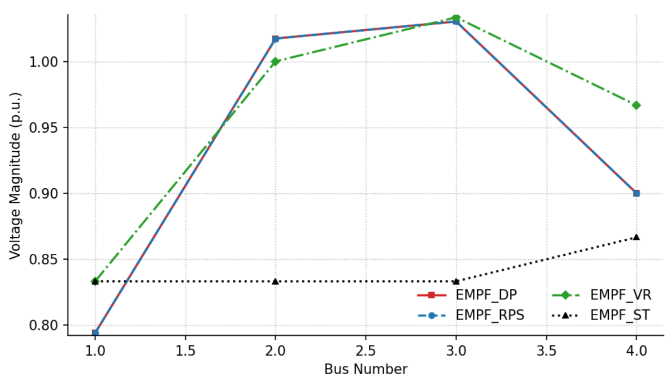

Fig. 3. Voltage magnitude profile vs. bus index for four control modes: DP, RPS, VR, and ST.

V. CONCLUSION

This paper presented a quantum-augmented, three-phase unbalanced power flow framework that explicitly incorporates hierarchically controlled grid-forming (GFM) inverters. The classical linear solve in the Newton step was replaced and introduce a Hermitian-embedded Variational Quantum Linear Solver (VQLS), yielding a formulation that is compatible with noisy. Numerical studies on the IEEE 4-node unbalanced feeder show that the proposed QPF reproduces the same voltage profiles, phase angles, and droop-controlled behavior as the classical Newton solver, with matching iteration counts and residual norms. At the same time, the VQLS implementation provides access to additional diagnostics such as linear residuals and probability distributions of bus voltages, offering new insight into solver behavior on a quantum backend. These results indicate that quantum-enhanced three-phase power flow with hierarchical GFM control is feasible on small systems today and can serve as a building block for future large-scale, real-time distribution system applications as quantum hardware matures.

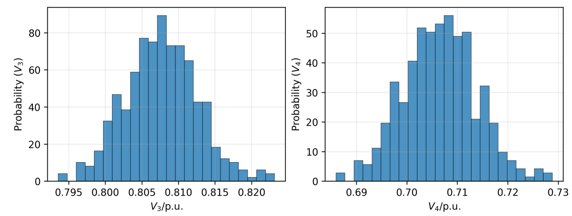

((a)) Voltage results calculated using classical solver.

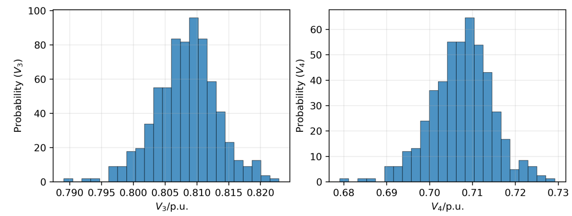

((b)) Voltage results calculated using QPF–VQLS.

Fig. 4. Probability distributions of voltage magnitudes at Buses 2 and 4.

REFERENCES

[1] P. A. N. Garcia, J. L. R. Pereira, S. Carneiro, Jr., V. M. da Costa, and N. Martins, "Three-Phase Power Flow Calculations Using the Current Injection Method," IEEE Transactions on Power Systems, vol. 15, no. 2, pp. 508–514, May 2000.

[2] Y. Zhou, Z. Tang, N. Nikmehr, P. Babahajiani, F. Feng, T.-C. Wei, H. Zheng, and P. Zhang, "Quantum computing in power systems," iEnergy, vol. 1, no. 2, pp. 170–187, Jun. 2022.

[3] B. Sævarsson, S. Chatzivasileiadis, H. Jóhannsson, and J. Østergaard, "Quantum Computing for Power Flow Algorithms: Testing on real Quantum Computers," in Proc. 11th Bulk Power Systems Dynamics and Control Symposium (IREP), Banff, Canada, Jul. 25–30, 2022.

[4] F. Feng, Y. Zhou, and P. Zhang, "Quantum Power Flow," arXiv:2104.04888 [quant-ph], Apr. 2021.

[5] F. Feng, Y. Zhou, and P. Zhang, "Noise-resilient quantum power flow," iEnergy, vol. 2, no. 1, pp. 63–70, Mar. 2023.

[6] S. Golestan, M. R. Habibi, S. Y. Mousazadeh Mousavi, J. M. Guerrero, and J. C. Vasquez, "Quantum computation in power systems: An overview of recent advances," Energy Reports, 2023.

[7] F. Feng, P. Zhang, Y. Zhou, and Y. A. Shamash, "Noisy-intermediate-scale quantum power system state estimation," iEnergy, vol. 3, no. 3, pp. 135–141, Sep. 2024.

[8] B. Sereeter, K. Vuik, and C. Witteveen, "Newton Power Flow Methods for Unbalanced Three-Phase Distribution Networks," Energies, vol. 10, no. 10, Art. no. 1658, Oct. 2017.

[9] S. Mossing, O. Amestegui, M. Jonas, F. Feng, L. Wang, Q. Shen, S. Zarrabian, Z. Liu, and P. Zhang, "Generalized shipboard microgrid power flow incorporating hierarchical control," iEnergy, vol. 4, no. 3, pp. 165–173, Aug. 2025.

[10] L. Hakim, M. Wahidi, U. Murdika, F. Milano, J. Kubokawa and N. Yorino, "A three-phase power flow analysis for electrical power distribution system with low voltage profile," 2015 2nd International Conference on Information Technology, Computer, and Electrical Engineering (ICITACEE), Semarang, Indonesia, 2015 .

[11] F. Feng, Y. -F. Zhou and P. Zhang, "Noise-resilient quantum power flow," in iEnergy, vol. 2, no. 1, pp. 63-70, March 2023.

[12] K. P. Schneider, B. A. Mather, B. C. Pal, C. W. Ten, G. J. Shirek, H. Zhu, J. C. Fuller, J. L. R. Pereira, L. F. Ochoa, S. Matthias, S. Paudyal, T. E. McDermott, and W Kersting, "Analytic Considerations and Design Basis for the IEEE Distribution Test Feeders," IEEE Transactions on Power Systems, vol. PP, no. 99, pp. 1-1, 2017.

979-8-3315-8138-1